# Searches for periodic neutrino emission from binary systems with 22 and 40 strings of IceCube

IceCube Collaboration: R. Abbasi[1], Y. Abdou[2], T. Abu-Zayyad[3], M. Ackermann[4], J. Adams[5], J. A. Aguilar[1], M. Ahlers[6], M. M. Allen[7], D. Altmann[8], K. Andeen[1,9], J. Auffenberg[10], X. Bai[11,12], M. Baker[1], S. W. Barwick[13], R. Bay[14], J. L. Bazo Alba[4], K. Beattie[15], J. J. Beatty[16,17], S. Bechet[18], J. K. Becker[19], K.-H. Becker[10], M. L. Benabderrahmane[4], S. BenZvi[1], J. Berdermann[4], P. Berghaus[11], D. Berley[20], E. Bernardini[4], D. Bertrand[18], D. Z. Besson[21], D. Bindig[10], M. Bissok[8], E. Blaufuss[20], J. Blumenthal[8], D. J. Boersma[8], C. Bohm[22], D. Bose[23], S. Böser[24], O. Botner[25], A. M. Brown[5], S. Buitink[23], K. S. Caballero-Mora[7], M. Carson[2], D. Chirkin[1], B. Christy[20], F. Clevermann[26], S. Cohen[27], C. Colnard[28], D. F. Cowen[7,29], A. H. Cruz Silva[4], M. V. D'Agostino[14], M. Danninger[22], J. Daughhetee[30], J. C. Davis[16], C. De Clercq[23], T. Degner[24], L. Demirörs[27], F. Descamps[2], P. Desiati[1], G. de Vries-Uiterweerd[2], T. DeYoung[7], J. C. Díaz-Vélez[1], M. Dierckxsens[18], J. Dreyer[19], J. P. Dumm[1], M. Dunkman[7], J. Eisch[1], R. W. Ellsworth[20], O. Engdegård[25], S. Euler[8], P. A. Evenson[11], O. Fadiran[1], A. R. Fazely[31], A. Fedynitch[19], J. Feintzeig[1], T. Feusels[2], K. Filimonov[14], C. Finley[22], T. Fischer-Wasels[10], B. D. Fox[7], A. Franckowiak[24], R. Franke[4], T. K. Gaisser[11], J. Gallagher[32], L. Gerhardt[15,14], L. Gladstone[1], T. Glüsenkamp[4], A. Goldschmidt[15], J. A. Goodman[20], D. Góra[4], D. Grant[33], T. Griesel[34], A. Groß[5,28], S. Grullon[1], M. Gurtner[10], C. Ha[7], A. Haj Ismail[2], A. Hallgren[25], F. Halzen[1], K. Han[4], K. Hanson[18,1], D. Heinen[8], K. Helbing[10], R. Hellauer[20], S. Hickford[5], G. C. Hill[1], K. D. Hoffman[20], B. Hoffmann[8], A. Homeier[24], K. Hoshina[1], W. Huelsnitz[20,35], J.-P. Hülß[8], P. O. Hulth[22], K. Hultqvist[22], S. Hussain[11], A. Ishihara[36], E. Jacobi[4], J. Jacobsen[1], G. S. Japaridze[37], H. Johansson[22], K.-H. Kampert[10], A. Kappes[38], T. Karg[10], A. Karle[1], P. Kenny[21], J. Kiryluk[15,14], F. Kislat[4], S. R. Klein[15,14], J.-H. Köhne[26], G. Kohnen[39], H. Kolanoski[38], L. Köpke[34], S. Kopper[10], D. J. Koskinen[7], M. Kowalski[24], T. Kowarik[34],

M. Krasberg[1], G. Kroll[34], N. Kurahashi[1], T. Kuwabara[11], M. Labare[23], K. Laihem[8], H. Landsman[1], M. J. Larson[7], R. Lauer[4], J. Lünemann[34], J. Madsen[3], A. Marotta[18], R. Maruyama[1], K. Mase[36], H. S. Matis[15], K. Meagher[20], M. Merck[1], P. Mészáros[29,7], T. Meures[18], S. Miarecki[15,14], E. Middell[4], N. Milke[26], J. Miller[25], T. Montaruli[1,40], R. Morse[1], S. M. Movit[29], R. Nahnhauer[4], J. W. Nam[13], U. Naumann[10], D. R. Nygren[15], S. Odrowski[28], A. Olivas[20], M. Olivo[19], A. O'Murchadha[1], S. Panknin[24], L. Paul[8], C. Pérez de los Heros[25], J. Petrovic[18], A. Piegsa[34], D. Pieloth[26], R. Porrata[14], J. Posselt[10], P. B. Price[14], G. T. Przybylski[15], K. Rawlins[41], P. Redl[20], E. Resconi[28,42], W. Rhode[26], M. Ribordy[27], M. Richman[20], J. P. Rodrigues[1], F. Rothmaier[34], C. Rott[16], T. Ruhe[26], D. Rutledge[7], B. Ruzybayev[11], D. Ryckbosch[2], H.-G. Sander[34], M. Santander[1], S. Sarkar[6], K. Schatto[34], T. Schmidt[20], A. Schönwald[4], A. Schukraft[8], A. Schultes[10], O. Schulz[28,43], M. Schunck[8], D. Seckel[11], B. Semburg[10], S. H. Seo[22], Y. Sestayo[28], S. Seunarine[44], A. Silvestri[13], G. M. Spiczak[3], C. Spiering[4], M. Stamatikos[16,45], T. Stanev[11], T. Stezelberger[15], R. G. Stokstad[15], A. Stößl[4], E. A. Strahler[23], R. Ström[25], M. Stüer[24], G. W. Sullivan[20], Q. Swillens[18], H. Taavola[25], I. Taboada[30], A. Tamburro[3], A. Tepe[30], S. Ter-Antonyan[31], S. Tilav[11], P. A. Toale[46], S. Toscano[1], D. Tosi[4], N. van Eijndhoven[23], J. Vandenbroucke[14], A. Van Overloop[2], J. van Santen[1], M. Vehring[8], M. Voge[24], C. Walck[22], T. Waldenmaier[38], M. Wallraff[8], M. Walter[4], Ch. Weaver[1], C. Wendt[1], S. Westerhoff[1], N. Whitehorn[1], K. Wiebe[34], C. H. Wiebusch[8], D. R. Williams[46], R. Wischnewski[4], H. Wissing[20], M. Wolf[28], T. R. Wood[33], K. Woschnagg[14], C. Xu[11], D. L. Xu[46], X. W. Xu[31], J. P. Yanez[4], G. Yodh[13], S. Yoshida[36], P. Zarzhitsky[46], and M. Zoll[22]

[1]Dept. of Physics, University of Wisconsin, Madison, WI 53706, USA

[2]Dept. of Physics and Astronomy, University of Gent, B-9000 Gent, Belgium

[3]Dept. of Physics, University of Wisconsin, River Falls, WI 54022, USA

[4]DESY, D-15735 Zeuthen, Germany

[5]Dept. of Physics and Astronomy, University of Canterbury, Private Bag 4800, Christchurch, New Zealand

[6]Dept. of Physics, University of Oxford, 1 Keble Road, Oxford OX1 3NP, UK

[7]Dept. of Physics, Pennsylvania State University, University Park, PA 16802, USA

[8]III. Physikalisches Institut, RWTH Aachen University, D-52056 Aachen, Germany

[9]now at Dept. of Physics and Astronomy, Rutgers University, Piscataway, NJ 08854, USA

[10]Dept. of Physics, University of Wuppertal, D-42119 Wuppertal, Germany

[11]Bartol Research Institute and Department of Physics and Astronomy, University of Delaware, Newark, DE 19716, USA

[12]now at Physics Department, South Dakota School of Mines and Technology, Rapid City, SD 57701, USA

[13]Dept. of Physics and Astronomy, University of California, Irvine, CA 92697, USA

[14]Dept. of Physics, University of California, Berkeley, CA 94720, USA

[15]Lawrence Berkeley National Laboratory, Berkeley, CA 94720, USA

[16]Dept. of Physics and Center for Cosmology and Astro-Particle Physics, Ohio State University, Columbus, OH 43210, USA

[17]Dept. of Astronomy, Ohio State University, Columbus, OH 43210, USA

[18]Université Libre de Bruxelles, Science Faculty CP230, B-1050 Brussels, Belgium

[19]Fakultät für Physik & Astronomie, Ruhr-Universität Bochum, D-44780 Bochum, Germany

[20]Dept. of Physics, University of Maryland, College Park, MD 20742, USA

[21]Dept. of Physics and Astronomy, University of Kansas, Lawrence, KS 66045, USA

[22]Oskar Klein Centre and Dept. of Physics, Stockholm University, SE-10691 Stockholm, Sweden

[23]Vrije Universiteit Brussel, Dienst ELEM, B-1050 Brussels, Belgium

[24]Physikalisches Institut, Universität Bonn, Nussallee 12, D-53115 Bonn, Germany

[25]Dept. of Physics and Astronomy, Uppsala University, Box 516, S-75120 Uppsala, Sweden

[26]Dept. of Physics, TU Dortmund University, D-44221 Dortmund, Germany

[27]Laboratory for High Energy Physics, École Polytechnique Fédérale, CH-1015 Lausanne, Switzerland

[28]Max-Planck-Institut für Kernphysik, D-69177 Heidelberg, Germany

[29]Dept. of Astronomy and Astrophysics, Pennsylvania State University, University Park, PA 16802, USA

[30]School of Physics and Center for Relativistic Astrophysics, Georgia Institute of Technology, Atlanta, GA 30332, USA

[31]Dept. of Physics, Southern University, Baton Rouge, LA 70813, USA

[32]Dept. of Astronomy, University of Wisconsin, Madison, WI 53706, USA

[33]Dept. of Physics, University of Alberta, Edmonton, Alberta, Canada T6G 2G7

[34]Institute of Physics, University of Mainz, Staudinger Weg 7, D-55099 Mainz, Germany

[35]Los Alamos National Laboratory, Los Alamos, NM 87545, USA

[36]Dept. of Physics, Chiba University, Chiba 263-8522, Japan

[37]CTSPS, Clark-Atlanta University, Atlanta, GA 30314, USA

[38]Institut für Physik, Humboldt-Universität zu Berlin, D-12489 Berlin, Germany

[39]Université de Mons, 7000 Mons, Belgium

[40]also Sezione INFN, Dipartimento di Fisica, I-70126, Bari, Italy

[41]Dept. of Physics and Astronomy, University of Alaska Anchorage, 3211 Providence Dr.,

Received _____; accepted _____

Anchorage, AK 99508, USA

[42]now at T.U. Munich, 85748 Garching & Friedrich-Alexander Universität Erlangen-Nürnberg, 91058 Erlangen, Germany

[43]now at T.U. Munich, 85748 Garching, Germany

[44]Dept. of Physics, University of the West Indies, Cave Hill Campus, Bridgetown BB11000, Barbados

[45]NASA Goddard Space Flight Center, Greenbelt, MD 20771, USA

[46]Dept. of Physics and Astronomy, University of Alabama, Tuscaloosa, AL 35487, USA

## ABSTRACT

Recent observations of GeV/TeV photon emission from several X-ray binaries have sparked a renewed interest in these objects as galactic particle accelerators. In spite of the available multi-wavelength data, their acceleration mechanisms are not determined, and the nature of the accelerated particles (hadrons or leptons) is unknown. While much evidence favors leptonic emission, it is very likely that a hadronic component is also accelerated in the jets of these binary systems. The observation of neutrino emission would be clear evidence for the presence of a hadronic component in the outflow of these sources.

In this paper we look for periodic neutrino emission from binary systems. Such modulation, observed in the photon flux, would be caused by the geometry of these systems. The results of two searches are presented that differ in the treatment of the spectral shape and phase of the emission. The 'generic' search allows parameters to vary freely and best fit values, in a 'model-dependent' search, predictions are used to constrain these parameters.

We use the IceCube data taken from May 31, 2007 to April 5, 2008 with its 22-string configuration, and from April 5, 2008 and May 20, 2009 with its 40-string configuration. For the generic search and the 40 string sample, we find that the most significant source in the catalog of 7 binary stars is Cygnus X-3 with a 1.8% probability after trials ($2.1\,\sigma$ one-sided) of being produced by statistical fluctuations of the background. The model-dependent method tested a range of system geometries — the inclination and the massive star's disk size — for LS I $+61^\circ$ 303, no significant excess was found.

## 1. Introduction

Recently, the observation of Very High Energy (VHE) $\gamma$-ray emission from several high mass X-ray binaries has established a new subclass of VHE or "$\gamma$-ray-loud" binaries. Gamma-rays are particularly interesting for neutrino searches because they can both produced by pion decays in an hadronic scenario. Three such systems, PSR B1259-63, LS 5039, and LS I +61° 303, have been identified as persistent TeV $\gamma$-ray emitters, while two others, Cygnus X-1 and HESS J0632+057, are possible candidates. PSR B1259-63 (Aharonian et al. 2005a) is formed by a B2Ve star orbited by a young 48 ms pulsar (Tavani & Arons 1997) both exhibiting a strong wind. As observed in (Aharonian et al. 2005a), its VHE emission could come from Inverse Compton scattering on shock-accelerated leptons from the interaction zone between the pulsar and wind from the star though a hadronic interpretation cannot be excluded. On the other hand, the driving factor of the VHE emission in Cygnus X-1, most probably a black hole orbiting a super-giant O9.7 star (Ziółkowski 2005), could be the interaction of the black hole with the strong stellar wind of the star. However, there has been no other evidence for steady VHE emission of Cygnus X-1, though a VHE flare of about 1 h was observed (Albert et al. 2007).

LS I +61° 303 remains a mystery even after four decades of observations over a wide range of wavelengths, from radio (Gregory et al. 1979), soft and hard X-ray (Harrison et al. 2000; Sidoli et al. 2006), GeV (Abdo et al. 2009a) and TeV photons (Albert et al. 2009; Acciari et al. 2009). The best measurement of its period, $P_1 = 26.4960 \pm 0.0028$ d, comes from radio data (Gregory et al. 1999) with the orbital zero phase taken at JD 2443366.775 (Gregory & Taylor 1978), but the same modulation has also been detected in other wavelengths, notably in the GeV/TeV band emission (Abdo et al. 2009a; Albert et al. 2009). The optical component, a massive, rapidly rotating B0Ve main sequence star loses mass through a strong stellar wind thought to be formed by a fast, low-density polar wind and a slow, high-density equatorial decretion disc (Romero et al. 2007). Yet, the nature of

the compact companion cannot be constrained to exclude either a neutron star or a black hole (Sierpowska-Bartosik & Torres 2009). It remains open if the VHE emission stems from a microquasar scenario (Bosch-Ramon et al. 2006b) or a pulsar scenario (Dubus et al. 2010). A similar argument (Paredes et al. 2000; Casares et al. 2005; Ribó et al. 2008) can be made for LS 5039 which was discovered in the TeV $\gamma$ band shortly after PSR B1259-63 (Aharonian et al. 2005b). As a consequence of our poor knowledge of the accelerator, the composition of the outflow is unknown. Existing observations cannot exclude the presence of hadrons in the pulsar wind. The observation of multi-TeV neutrinos would unequivocally prove the existence of hadronic acceleration.

The paper is organized as follows. In Section 2 we describe the IceCube observatory and the data taken with two detector configurations (Achterberg et al. 2006). The analysis method is described in Sec. 3. The underlying hypothesis of the adopted likelihood method is that the neutrino emission is periodically modulated due to the geometry of the considered X-ray binaries. Neutrinos would be produced by a beam of hadrons accelerated by the compact object and interacting with the matter of the massive star and its atmosphere. The periodic modulation would be connected to the rotation of the system. This modulation is observed in photons from radio to X-ray, and in the VHE. While the signal is modulated in time, the background of atmospheric and muon neutrinos is random in time. Hence, it is estimated scrambling data in time – each scrambled data set is equivalent to a sample of atmospheric background. In the sections that follow, the search method, its expected discovery potential, and results are illustrated. To avoid any bias toward discovery, each search has been performed in a blind fashion by defining cuts before looking at the time (or right ascension) of the final event sample. The post-trial p-values are robust, since we use data themselves to estimate the background.

Section 4 describes the first search, called hereafter 'generic', since it incorporates only minimal assumptions regarding the neutrino spectrum: a simple power law emission

spectrum and a period that matches the periodicity in an observed electromagnetic wavelength. The phase of the neutrino flux is not constrained to match the phase of the observed photon emission. It is instead a free parameter of a fit to account for the fact that photons can be absorbed when the accelerator is behind the large star of the binary system while neutrino production can be enhanced if enough matter is crossed. The search catalog consists of 7 galactic binary stars in the Northern sky. The selected objects are considered as microquasars in Distefano et al. (2002), where their expected emission of neutrinos is calculated. That paper is not specifically on the periodic emission of these sources, nonetheless the objects considered there are promising neutrino emitters for which radio observations allow identification of jet parameters such as the Lorentz factor and the luminosity of the jet. All the considered sources are located in the Northern Hemisphere, since in this region IceCube is more sensitive to sources in the TeV-PeV region (Abbasi et al. 2011).

A model-dependent search was also carried out (Section 5) for LS I +61° 303. The serach relies on phenomenological predictions for the spectral neutrino light curve (SNLC). This places constraints on the nuisance parameters of this search, e.g. the spectral index of the neutrino emission and its phase. For LS I +61° 303, several time-integrated flux predictions that would lead to a detection of neutrinos in an IceCube-like detector exist (Distefano et al. 2002; Christiansen et al. 2006), and some authors predict a SNLC (Torres & Halzen 2007; Orellana & Romero 2007). The prediction used here is based on the emission model first mentioned in Neronov & Ribordy (2009) and developed into an SNLC in Chernyakova et al. (2009). In this model, the dense stellar disk that is formed by the outflow of the massive Be star is assumed to be oriented perpendicularly to the observer's line of sight, so that the orbital phase period in which the compact object stays behind the massive star is maximal. The compact object's relativistic outflow delivers high energy protons that are only weakly deflected in the system's magnetic field — literature gives

estimates between $0.2 - 0.35\,\mathrm{G}$ (Chernyakova et al. 2006) and $1\,\mathrm{G}$ (Bosch-Ramon et al. 2006a) — so that their Larmor radius at several PeV is comparable to the size of the system. The interaction of these protons with the dense stellar disk subsequently emits a neutrino flux into a cone that is aligned with the axis of the compact object – Be star system. The resulting neutrino flux can only be observed if the compact object is eclipsed by the dense stellar disk with respect to the observer. The neutrino emission windows predicted by this geometric model occur before the periastron and are therefore not in phase with the emission maxima observed in the GeV and TeV bands, which peak at phases around 0.3-0.4 (GeV band) and 0.7-0.8 (TeV band). The $\gamma$-ray emission from secondary $e^{\pm}$ and $\pi^0$ decay that accompanies the neutrino emission will be strongly suppressed due to the high density of soft photons and matter in the dense stellar disk, delaying the onset of the GeV emission peak. As a consequence, Chernyakova et al. (2009) does not give a prediction for the neutrino flux normalization within their time-dependent emission model.

## 2. The IceCube data

Construction of the IceCube Neutrino Observatory started with a first string installed in the austral season of 2005/2006 (Achterberg et al. 2006) and was completed in December 2010. It is composed of an array of 86 strings with a total of 5160 Digital Optical Modules (DOMs) instrumented between a depth of 1,450 and 2,450 m. The deep ice detector is complemented at the surface by the extensive air shower array IceTop. Each DOM consists of a 25 cm diameter Hamamatsu photomultiplier (Abbasi et al. 2010a), electronics to digitize the PMT output voltage (Abbasi et al. 2009b) and all in a spherical, pressure-resistant glass housing. IceCube observes the Cherenkov light emitted by relativistic charged particles produced in high-energy neutrino interactions. The PMT signals are digitized and the charge and arrival time of photons measured. The data taking and performances of the detector are described in Abbasi et al. (2011). IceCube triggers primarily on down-going

muons: in the 40-string configuration at a rate of about 950 Hz and in the 22-string configuration at about 350 Hz. During the austral summer the atmosphere above the South Pole gets warmer and thinner and the probability of pions generated in cosmic ray air showers to decay rather than interact increases (Tilav et al. 2009), causing the trigger rate to vary by about $\pm 10\%$. At final level of analysis, dominated by upwardgoing atmospheric neutrinos, events come from many different directions. Hence, temperature effects average over a wide terrestrial region and the seasonal modulation is only a few percent. In any case, this variation has a period of one year, much longer than any period considered in this search.

The searches presented here used two data samples. The data taken with the 22-string configuration have a livetime of 275.7 days, or a total livetime of 89% of the operation period from May 31, 2007 to April 5, 2008 (MJD 54251-54561). The sample is described in Abbasi et al. (2009a), and consists of 5114 events, which are mostly neutrino induced upward-going muons with declinations from -5° to +85°. The deadtime is mainly due to test and calibration runs during and after the construction season. The 22-string data sample has been unblinded for discovery for the generic search, and for the model-dependent search it was used for establishing the methodology and provide an *a posteriori* p-value. Both methods were then applied on data taken with the 40-string configuration for discovery. The lifetime of the 40-string data used in analysis is 375.7 d which is 92% of the nominal operation period from April 5, 2008 to May 20, 2009 or Modified Julian Day (MJD) 54561-54971. The handling and processing of the data to obtain the final neutrino candidate event sample are fully discussed in Abbasi et al. (2011). The final 40-string sample contains 36,900 atmospheric neutrino and muon events distributed over the whole sky, of which 14,121 events are up-going, and 22,779 events are down-going. The median angular resolution for the final samples of the analysis for energies larger than 10 TeV is below $1^o$. About 50% of the reconstructed muon events produced by neutrinos with

energy between 10-100 TeV (1-10 PeV) from a direction are inside $1^o$ ($0.6^o$). The selected atmospheric neutrino events are in the TeV-PeV range in the up-going region, while in the down-going region a high energy sample of PeV-EeV atmospheric muons is selected. This difference in sensitivity is due to the need of reducing the large number of downgoing muon events that not only would mask the neutrino signal but that are too numerous to apply the time-consuming likelihood method to build the full skymaps. For this scope, a zenith-dependent energy proxy cut has been implemented to reduce the muon event rate to roughly that of the atmospheric neutrino background used for the point-source search in the northern hemisphere. This energy proxy uses the density of photons along the muon track due to stochastic energy losses of pair production, bremsstrahlung and photonuclear interactions which dominate over ionization losses for muons above 1 TeV. The achieved energy resolution is about 0.3 in $\log_{10}$ of the muon energy in the detector between 10 TeV and $10^5$ TeV. The muon neutrino flux upper limits at 90% CL for time-independent searches (depending on declination) are between $E^2 dN/dE \sim 3 - 20 \times 10^{-12}\,\mathrm{TeV\,cm^{-2}\,s^{-1}}$ in the northern sky where the sources considered in this paper are located.

The 22 and 40-string data samples used in this paper were also used to look for bursting neutrino sources in (Abbasi et al. 2010b) where the stability of the data taking is discussed in detail. Azimuthal geometry effects of the 40 and 22-string IceCube detectors (due to the fact that they are more elongated in one direction than in others) and rotation of the Earth interfere constructively for source periods with a multiple of one half of a day, which is not the case for any of the source periods tested.

The limits in this paper were produced assuming a flux of only muon neutrinos at the Earth with simulated energies from $10^8$ to $10^{19}$ eV. For standard neutrino oscillations over astronomical distances (Athar et al. 2000), equal fluxes of all neutrino flavors at the Earth are expected from a source producing neutrinos via pion decay with a ratio of $\nu_e : \nu_\mu : \nu_\tau = 1 : 2 : 0$. For the assumption of equal fluxes of muon and tau neutrinos at the

Earth, the resulting upper limits on the sum of both fluxes are about 1.7 times higher than if only muon neutrinos are considered (Abbasi et al. 2011). This sets better limits than the expected factor of two due to oscillations if no tau neutrinos would be detectable. This is due to the tau decay channel into muons with a branching ratio of 17.7%. In addition to this, tau leptons with energy greater than some PeVs that may travel far enough to be reconstructed as tracks in IceCube before decaying. For an $E^{-2}$ neutrino spectrum the contribution due to the detectable tau neutrino flux for sources at the horizon is 10% and rising to 15% for sources in the Northern hemisphere.

The main systematic uncertainties on the flux upper limits come from photon propagation in ice, absolute DOM efficiency, and uncertainties in the Earth density profile and muon energy loss. For an $E^{-2}$ spectrum the estimated total uncertainty is about 16% (Abbasi et al. 2011). They are included in the upper limits calculations following the method of Conrad et al. (2003) with the modification described in Hill (2003).

## 3. Method

The generic and model dependent searches presented here both use a likelihood method. The method was extensively described in Braun et al. (2008, 2010). The generic search requires no binning in the used variables, while the model dependent search selected events within an angular window from the source and with a cut on an energy proxy. In the likelihood ratio method, the data are modeled as a combination of signal and background populations. In the absence of detector biases, the background is randomly distributed in time, whereas the signal will have periodic features. Hence, the p-value of the results are calculated by comparing to the fraction of scrambled trials in right ascension (equivalent to time) which have a larger likelihood ratio than what found in data. The probability density function of the background and of the signal contains three terms: a space term, an

energy term and a time dependent term. The first two are described in detail in (Abbasi et al. 2011). The first term characterizes the signal of a point source as clustered around its direction with an angular spread mainly due to the angular error of the reconstruction. The second is used because the signal is expected to have harder spectra than the background. Below we will discuss each time dependent term used in the searches presented here. The generic search describes the shape of the periodic emission as a Gaussian. The model dependent search uses a rectangular window in time. In the generic method the spectral index is a freely fit parameter while the model-dependent method uses assumed spectra from models.

We calculate the sensitivity and median upper limit at 90% confidence level using the method of Feldman & Cousins (Feldman & Cousins 1998). A discovery potential is calculated as the flux required to achieve a p-value less than $2.87\times10^{-7}$ ($5\sigma$ of the upper tail of a one-sided Gaussian) in 50% of trials. It should be noted that the threshold significance to claim a discovery in IceCube is set to $5\sigma$. Fig. 1 shows the sensitivity and the discovery potential for the two methods, together with the corresponding values from the time-integrated search (Abbasi et al. 2009a).

## 4. Generic periodic emission search

Inspired by the periodic modulation of the photon emission in the TeV and GeV $\gamma$ bands that has been observed for LS I $+61^\circ$ 303 (Albert et al. 2006; Abdo et al. 2009a), this search is extended to other microquasars and binary systems. The modulation in the LS I $+61^\circ$ 303 emission is interpreted as an indication of the absorption of $\gamma$-rays in the system depending on the relative position of the observer and the accelerator. We assume that the neutrino emission period is the same as for photons, but in this generic search we leave the phase as a free parameter in our method to be sensitive to possible shifts in phase

between neutrinos and photons.

The best fit values for the signal fraction, spectral index, and the peak phase and duration of neutrino emission are obtained by maximizing the likelihood ratio. For the signal hypothesis, a Gaussian emission repeating each orbit is assumed. Hence our time-dependent pdf is:

$$S_i^{\text{time}} = \frac{1}{\sqrt{2\pi}\sigma_T} e^{-\frac{|\varphi_i - \varphi_0|^2}{2\sigma_T^2}}, \tag{1}$$

where $\sigma_T$ is the width of the Gaussian, $\varphi_i$ is the phase of the event and $\varphi_0$ is the phase of the peak of the emission. The fit parameters are $\sigma_T$ and $\varphi_0$.

Comparing to the unbinned time-integrated analysis, we find that searching for periodicity in neutrino emission results in a better discovery potential if the duration of the emission $\sigma_T$ is less than about 20% of the total period (see Fig. 1). As the time-dependent search adds two additional degrees of freedom to the analysis, the discovery potential is roughly 10-15% worse if neutrinos are actually emitted at a steady rate or over a large fraction of the period. For both the case of 22 strings and 40 strings (see Fig. 1), if the emission has a $\sigma_T$ of 1/50 of the period the method requires about half as many events for discovery than the time-independent search.

### 4.1. Results

The seven predefined sources, listed in Table 1, were used for this search with the 22-string sample. There was no evidence of periodicity seen for any of the sources tested. The most significant result for this sample was the source SS 433, with a pre-trial p-value of 6%, which we expect to see from at least one of our seven tested sources in 35% of background-only scrambled samples.

For the subsequent 40-string configuration, the most significant deviation from the

background only hypothesis is for Cygnus X-3. The pretrial p-value of this source is 0.00186, where an equivalent best p-value from any of the sources is found in 1.8% of scrambled samples, so the result is compatible with random fluctuations. The peak emission is found to be at phase $\hat{\varphi}_0 = 0.8$, and $\hat{\sigma}_T = 0.02$. The best-fit number of source events is $\hat{n}_s = 4.28$ and spectrum is soft at $\hat{\gamma}_s = 3.75$. In a one-degree bin centered on Cygnus X-3, 4 events are observed with a mean background of 1.9 events.

Fig. 2 compares the 40-string time-integrated limits to the model predictions in Distefano et al. (2002) for each source. The model predicts the neutrino flux based on the radiative luminosity associated to the jet from radio observations in quiescent states and during flares the duration of which is specified in Tab. 4 in that paper. The figure shows limits for both the persistent and time-dependent cases for a time window similar to the observed flare but not coincident to it (since IceCube was not active at the time of radio observations noted in the paper). For the persistent case of SS 433 the model predicts more than 100 events during the 40-string data taking period, which is excluded at greater than 99% condence level. It should be considered that the authors indicate in their paper that the model may be biassed by the fact that the source is surrounded by a the diffuse nebula W50 that can affect the estimate of the radio emission used in the model for SS 433.

The main parameters on which the neutrino flux depends in this model are: the fraction of jet kinetic energy converted to internal energy of electrons and magnetic field, $\eta_e$; the fraction of the jet luminosity carried by accelerated protons, $\eta_p$; and the fraction of proton energy in pions $f_\pi$, which strongly depends on the maximum energy to which protons can be accelerated. We show as an example for the case of a 3-day burst of Cygnus X-3 how the parameters are constrained by our result. We assume equipartition between the magnetic fields and the electrons and the proton component ($\eta_p = \eta_e$) for setting a constraint on $f_\pi < 0.11$. If equipartition does not apply, we assume $f_\pi = f_{\pi,peak}$ as given in Table 2 in Distefano et al. (2002) (for Cygnus X-3 $f_{\pi,peak} = 0.12$) and constrain $\eta_p$ to be

| Source | Period (days) | p-value (pretrial) | $T_0$ (MJD) | $\hat{\varphi}_o$ (phase) | $\hat{\sigma}_T$ (period$^{-1}$) | Reference | Time-Dependent UL (TeV$^{-1}$cm$^{-2}$s$^{-1}$) | Time-Integrated UL (TeV$^{-1}$cm$^{-2}$s$^{-1}$) |
|---|---|---|---|---|---|---|---|---|
| Cygnus X-3 | 0.199679 | 0.00186 | 53760.583997 | 0.819 | 0.02 | (Abdo et al. 2009b) | $3.01{\cdot}10^{-11}$ | $6.64{\cdot}10^{-12}$ |
| Cygnus X-1 | 5.5929 | 0.080 | 41874.707 | 0.031 | 0.02 | (Brocksopp et al. 1998) | $4.08{\cdot}10^{-12}$ | $7.41{\cdot}10^{-12}$ |
| LS I $+61^{\circ}$ 303 | 26.498 | 0.23 | 43366.775 | 0.916 | 0.02 | (Acciari et al. 2008) | $1.82{\cdot}10^{-11}$ | $9.78{\cdot}10^{-12}$ |
| GRS 1915+105 | 30.8 | 0.43 | 53945.7 | 0.502 | 0.045 | (Neil et al. 2007) | $2.57{\cdot}10^{-12}$ | $3.23{\cdot}10^{-12}$ |
| SS 433 | 13.0821 | 0.35 | 50023.62 | 0.779 | 0.02 | (Hillwig & Gies 2008) | $3.15{\cdot}10^{-12}$ | $3.03{\cdot}10^{-12}$ |
| XTE J1118+480 | 0.169934 | 0.28 | 52287.9929 | 0.985 | 0.132 | (McClintock et al. 2003) | $7.29{\cdot}10^{-12}$ | $8.18{\cdot}10^{-12}$ |
| GRO J0422+32 | 0.21214 | 0.037 | 50274.4156 | 0.831 | 0.02 | (Webb et al. 2000) | $1.46{\cdot}10^{-11}$ | $6.89{\cdot}10^{-12}$ |

Table 1:: System name, period, pre-trial p-value, and the time of zero phase for the binary systems tested. $\hat{\sigma}_T$ is the fraction of the standard deviation of the best-fit Gaussian of the period of the binary system. We also include the reference used for the orbital information. The last columns give the upper limits of Feldman-Cousins Feldman & Cousins (1998) 90% confidence intervals as the normalization on an $E^{-2}$ spectrum flux for the time-dependent and integrated hypotheses for the 40 strings data. The upper limits also incorporate a 16% systematic uncertainty.

less than 92% of $\eta_e$. In deriving these limits we have assumed that the Lorentz factor of the jet is well known from radio measurements, but in many cases there is a large uncertainty on this parameter. Hence, our limits to the parameters of this model may have different implications that we cannot disentangle: protons may not be dominant in the jet, they may lose smaller energies into pion decay than the values considered in Distefano et al. (2002), or the Lorentz factor is lower than the value indicated in Table 1 in that paper.

## 5. Time-dependent Search based on neutrino flux predictions for LS I +61° 303

In this section, we introduce a model-dependent search for a neutrino flux from LS I +61° 303. In contrast to the generic method discussed above, all nuisance parameters of this search are fixed according to model predictions from Neronov & Ribordy (2009); Chernyakova et al. (2009). The model allows to make predictions for the neutrino emission time window from the physical parameters of the binary system.

### 5.1. Phase Window Selection

The duration of the phase where observable neutrinos are emitted is given by the SNLC and depends on two parameters: the inclination $i$ of the system's ecliptic with respect to the observer, and the dimensionless radius $R/D_{\rm per}$ of its dense disk. The system's inclination is unknown and depends on the mass of its components. The favored mass interval of the optical star is $M_{\rm opt} = 10 - 15\,{\rm M}_\odot$ (Hutchings & Crampton 1981). With this constraint, Casares et al. (2005) conclude that the compact object would be a black hole for $i < 25°$, and a neutron star for $25° < i < 60°$.

In our choice of models, we consider an inclination of $i = 30°$, corresponding to the neutron star scenario with minimal mass ($1.4\,M_\odot$), with three different disk sizes

$R/D_{\rm per} = 1.0$, 1.5, and 2.0, and an inclination of $i = 10°$, corresponding to the black hole scenario with disk size $R/D_{\rm per} = 1.0$. $R/D_{\rm per}$ is equal to and larger than unity, in agreement with the limiting values discussed in (Sierpowska-Bartosik & Torres 2009). As discussed above, the time-dependent model lacks a more detailed SNLC prediction. Therefore, we consider a flat neutrino emission, i.e. constant within the allowed orbital phase range and, given the lack of a precise understanding of the acceleration mechanisms at the source, we consider simple power law neutrino spectra. Two spectral indices of $\gamma_s = 1.5$ or 2 were chosen: the latter represents Fermi acceleration-based models, whereas the former covers models with stronger acceleration mechanisms, e.g. acceleration in large scale electric fields. In summary, each model $M = M_{\gamma_s,i,R/D_{\rm per}}$ is characterized by the three physical parameters $i$, $R/D_{\rm per}$ and $\gamma_s$.

The bin size $\Psi$ and cut on the minimum reconstructed energy $E_{\rm cut}$ are optimized according to the model detection potential (MDP) (Hill et al. 2005) by minimizing a hypothetical flux for a $5\sigma$ discovery in 50% trials. Table 2 summarizes the results of the optimization for the 22-string data. The discovery potential is expressed in terms of the flux normalization $\Phi_0$ for a simple power law neutrino emission at the source. For this specific model, this approach is more sensitive than the generic one, although the differences are small (around 5% for the discovery potential, and 10% for the sensitivities).

The search was optimized for the 22-string data set in a blind fashion but treated as an *a posteriori* search. Therefore, a p-value can not be stated. We find the strongest fluctuation over background for the window Four event candidates remained after cuts on the time window, search bin radius and minimum energy proxy. They are all before or around the superior conjunction (at an orbital phase of 0.04). Based on this observation, an additional time window, "22-string best", was introduced to be tested for both spectral indices alongside the already introduced eight models. It allows neutrino emission between phases 0.9 and 1.1, giving a width of $\alpha_M = 0.2$ for the emission time window.

| Model $M_{\gamma_s,i,R/D_{\rm per}}$ | $(\varphi_{\rm min},\varphi_{\rm min})$ | $\Psi_{\rm opt}$ (deg) | log(EnergyProxy)$_{\rm cut}$ | $\alpha_M\mu_{\rm bg}$ | $\mu_{\rm lds}$ | $\Phi_0$ (TeV$^{-1}$cm$^{-2}$s$^{-1}$) |
|---|---|---|---|---|---|---|
| $M_{2,10,1.1}$ | (0.98, 1.20) | 2.6 | 2.0 | 1.2 | 7 | $4.2{\cdot}10^{-11}$ |
| $M_{2,10,1.5}/M_{2,30,2.0}$ | (0.93, 1.24) | 2.6 | 2.6 | 1.5 | 7 | $4.5{\cdot}10^{-11}$ |
| $M_{2,10,2.0}$ | (0.87, 1.24) | 2.4 | 2.2 | 1.6 | 8 | $4.8{\cdot}10^{-11}$ |
| $M_{2,30,1.5}$ | (1.01, 1.24) | 2.3 | 2.6 | 0.86 | 7 | $4.2{\cdot}10^{-11}$ |
| $M_{1.5,10,1.1}$ | (0.98, 1.20) | 2.6 | 2.8 | 0.92 | 5 | $5.6{\cdot}10^{-12}$ |
| $M_{1.5,10,1.5}/M_{1.5,30,2.0}$ | (0.93, 1.24) | 2.6 | 2.8 | 1.3 | 6 | $6.2{\cdot}10^{-12}$ |
| $M_{1.5,10,2.0}$ | (0.87, 1.24) | 2.6 | 2.8 | 1.6 | 6 | $6.4{\cdot}10^{-12}$ |
| $M_{1.5,30,1.5}$ | (1.01, 1.24) | 2.6 | 2.8 | 0.97 | 5 | $5.7{\cdot}10^{-12}$ |

Table 2:: Discovery potential for 22-string sample: a model is characterized by the inclination of the system w.r.t. the line of sight $i$, the disk size in periastron distance units $R/D_{\rm per}$ and the simple power law spectral index $\gamma_s$: $M_{\gamma_s,i,R/D_{\rm per}}$. $(\varphi_{\rm min},\ \varphi_{\rm max})$ are the beginning and the end of the neutrino emission time window, $\Psi$ and EnergyProxy$_{\rm cut}$ the optimal cut parameters, and $\alpha_M\mu_{\rm bg}$ the scaled average background expectation. A model leads to a $\geq 5\sigma$ CL detection in 50% of trials, if an average number of events $\mu_{\rm lds}$ is detected after final cuts. This corresponds to neutrino flux normalization $\Phi_0$ of a simple power law with spectral index $\gamma_s$ at the source, i.e. $\mathrm{d}\Phi/\mathrm{d}E = \Phi_0\,(E/\mathrm{TeV})^{-\gamma_s}$.

### 5.2. 40-string Application and Result

The search method presented so far was re-optimized and then unblinded on the 40-string data set. The best pre-trial p-value of 0.35 was obtained for model $M_{\rm IC22\ best,\ \gamma_s=2}$ with one event remaining in the final search window. Taking into account the trial factor for 10 simultaneous searches, the overall post-trial p-value is 65%, which is not significant. Table 3 summarizes the search parameters and the results for the time-dependent upper limit of the 90% CL Feldman-Cousins intervals.

| Model $M_{\gamma_s,i,R/D_{\rm per}}$ | $\Psi_{\rm opt}$ (deg) | log(EnergyProxy)$_{\rm cut}$ | $\alpha_M\mu_{\rm bg}$ | $n_s$ | p-value (pre-trial) | Time-Dependent Upper Limit (UL) ($\rm TeV^{-1}cm^{-2}s^{-1}$) |
|---|---|---|---|---|---|---|
| $M_{2,10,1.1}$ | 1.4 | 2.4 | 0.80 | 0 | 0.69 | $5.9{\cdot}10^{-12}$ |
| $M_{2,10,1.5}/M_{2,30,2.0}$ | 1.3 | 2.8 | 0.84 | 1 | 0.43 | $7.9{\cdot}10^{-12}$ |
| $M_{2,10,2.0}$ | 1.3 | 2.6 | 1.1 | 1 | 0.51 | $7.4{\cdot}10^{-12}$ |
| $M_{2,30,1.5}$ | 1.2 | 2.6 | 0.58 | 0 | 0.55 | $5.9{\cdot}10^{-12}$ |
| $M_{1.5,10,1.1}$ | 1.6 | 3.0 | 0.71 | 0 | 0.78 | $9.5{\cdot}10^{-13}$ |
| $M_{1.5,10,1.5}/M_{1.5,30,2.0}$ | 1.3 | 3.0 | 0.64 | 1 | 0.44 | $1.2{\cdot}10^{-12}$ |
| $M_{1.5,10,2.0}$ | 1.5 | 3.0 | 1.0 | 1 | 0.56 | $1.2{\cdot}10^{-12}$ |
| $M_{1.5,30,1.5}$ | 1.6 | 3.0 | 0.74 | 0 | 0.81 | $9.1{\cdot}10^{-13}$ |
| IC-22 best, $\gamma_s = 2$ | 1.4 | 2.4 | 0.70 | 1 | 0.36 | $8.6{\cdot}10^{-12}$ |
| IC-22 best, $\gamma_s = 1.5$ | 1.5 | 3.0 | 0.56 | 1 | 0.35 | $1.3{\cdot}10^{-12}$ |

Table 3:: Search results with 40-string data: A model is characterized by the inclination of the system w.r.t. the line of sight $i$, the disk size in periastron distance units $R/D_{\rm per}$ and the simple power law spectral index $\gamma_s$: $M_{\gamma_s,i,R/D_{\rm per}}$. $\Psi$ and log(EnergyProxy)$_{\rm cut}$ are the optimal cut parameters, and $\alpha_M\mu_{\rm bg}$ the scaled average background expectation. $n_s$ is the number of source events found in the respective time window after selection cuts that give the corresponding pre-trial p-value. The last column gives the upper limits of Feldman-Cousins 90% confidence intervals as the normalization on an $\rm E^{-2}$ spectrum flux.

## 6. Conclusions

The exploration of the GeV and TeV photon sky with the instruments on board the Fermi spacecraft and the ground-based Cherenkov telescopes has heralded the golden age of $\gamma$-ray astronomy. The connection to neutrino astronomy is clear: high energy processes which cause the observed VHE emission can be responsible for the observed high energy cosmic rays. This implies hadronic acceleration mechanisms in astrophysical sources which can result in an observable neutrino flux with giant neutrino telescopes like IceCube.

The available photon observations have made it possible to enhance the sensitivity of

searches for neutrino fluxes by incorporating assumptions derived from the $\gamma$-ray data. One crucial development has been the formulation of time-dependent neutrino flux searches, postulating a connection between the time modulation of the high energy emission and the possible neutrino flux. This assumption has increased the sensitivity of these searches in comparison to their time-averaged counterparts.

This paper presented two searches for neutrinos from objects with periodic photon/broadband emission. Seven X-ray binaries in the Northern Hemisphere were selected and tested with the generic method which scans the whole allowed neutrino spectrum parameter space. The most significant source in the catalog is Cygnus X-3 with a 1.8% probability after trials ($2.1\sigma$ one-sided). The best fit of the phase is 0.82, close to the superior conjunction of the system at phase = 0 and close to the peak of Fermi-LAT observations. Comparing the time-integrated limits for each source to model predictions from Distefano et al. (2002), the results exclude the prediction for SS 433 at greater than 99% confidence level. We show that our limits can constrain the fraction of jet luminosity which is converted into pions and the ratio of jet energy into relativistic leptons versus relativistic hadrons, under some assumptions. For instance, for Cygnus X-3 and equipartition between electrons and protons, the fraction of proton energy in pions is limited to about 11%.

The second method searched for a neutrino flux from LS I $+61^\circ$ 303 based on various predictions of the system parameters, i.e. size of the massive star's disk and the system's inclination. The most significant model prediction yielded a 35% (36%) probability before trials for an emission between the phases 0.9 and 1.1 with a spectral index of $\gamma_s = 1.5$ (2). The 90% CL Feldman–Cousin time-dependent upper limit is $1.3 \cdot 10^{-12}\,\mathrm{TeV}^{-1}\,\mathrm{cm}^{-2}\,\mathrm{s}^{-1}$ ($8.6{\cdot}10^{-12}\,\mathrm{TeV}^{-1}\,\mathrm{cm}^{-2}\,\mathrm{s}^{-1}$). Due to the geometric nature of the underlying model, no statement can be made with respect to the validity of the model predictions. However, these upper limits can guide further developments of models. LS I $+61^\circ$ 303 was also

included in the catalog of the generic search, with a pre-trial p-value of 23%. Its best fit phase of $\hat{\varphi}_0 = 0.92$ agrees well with the time window that gave the best p-value in the model-dependent search, $(0.9, 1.1)$. All of the results in this paper are compatible with a fluctuation of the background.

## 7. Acknowledgments

We thank D. Guetta and E. Waxman for helpful discussions on neutrino flux prediction models. We acknowledge the support from the following agencies: U.S. National Science Foundation-Office of Polar Programs, U.S. National Science Foundation-Physics Division, University of Wisconsin Alumni Research Foundation, the Grid Laboratory Of Wisconsin (GLOW) grid infrastructure at the University of Wisconsin - Madison, the Open Science Grid (OSG) grid infrastructure; U.S. Department of Energy, and National Energy Research Scientific Computing Center, the Louisiana Optical Network Initiative (LONI) grid computing resources; National Science and Engineering Research Council of Canada; Swedish Research Council, Swedish Polar Research Secretariat, Swedish National Infrastructure for Computing (SNIC), and Knut and Alice Wallenberg Foundation, Sweden; German Ministry for Education and Research (BMBF), Deutsche Forschungsgemeinschaft (DFG), Research Department of Plasmas with Complex Interactions (Bochum), Germany; Fund for Scientific Research (FNRS-FWO), FWO Odysseus programme, Flanders Institute to encourage scientific and technological research in industry (IWT), Belgian Federal Science Policy Office (Belspo); University of Oxford, United Kingdom; Marsden Fund, New Zealand; Japan Society for Promotion of Science (JSPS); the Swiss National Science Foundation (SNSF), Switzerland; A. Groß acknowledges support by the EU Marie Curie OIF Program; J. P. Rodrigues acknowledges support by the Capes Foundation, Ministry of Education of Brazil.

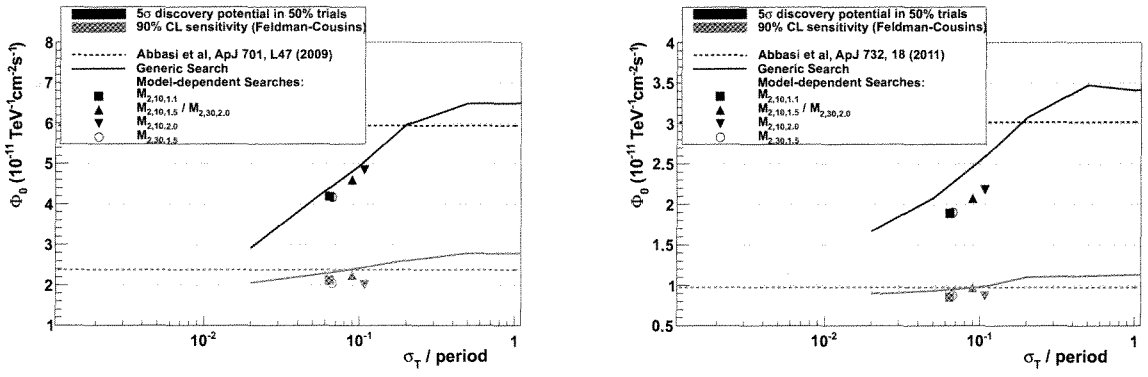


Fig. 1.—: Discovery potentials ($5\sigma$ in 50% trials, solid and dashed upper lines in the plot) and the average sensitivity at 90% CL calculated with the prescription in (Feldman & Cousins 1998) (solid and dashed lower lines) for the generic search applied to the 22-string data (left) and to the 40-string data (right). The y-axis shows the flux normalization $\Phi_0$ for a $E^{-2}$ simple power law spectrum emission from LS I $+61°$ 303 , i.e. $\mathrm{d}\Phi/\mathrm{d}E = \Phi_0\,(E/\mathrm{TeV})^{-2}$. The x-axis shows the width $\sigma_T$ of the Gaussian emission normalized to its period $P_1 = 26.4960\,\mathrm{d}$. Shown are the results for the time-integrated searches (Abbasi et al. 2009a, 2011) (dashed line) and for the generic time-dependent search (solid line). Symbols are the results for the model-dependent search (for comparison purposes in this plot, the rectangular time emission window otherwise used by the model-dependent search were converted into a Gaussian with the same normalization).

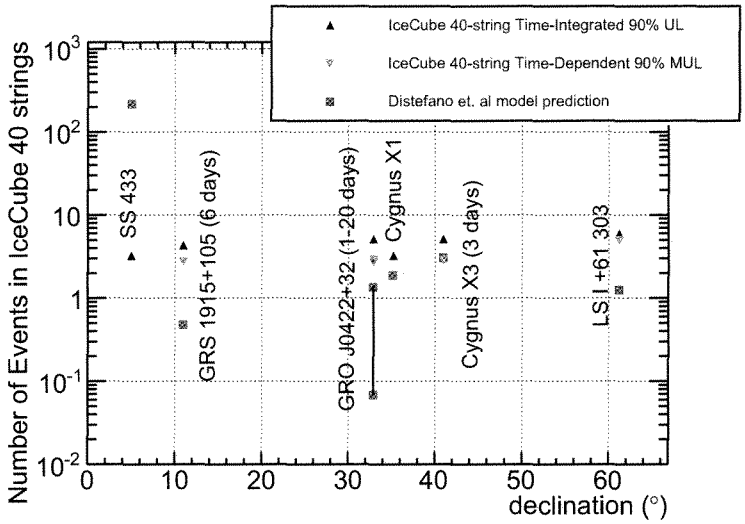


Fig. 2.—: The time-integrated upper limit (UL) at 90% CL on the number of events is compared to the expected number of events for model predictions according to Distefano et al. (2002) for specific sources for the 40 string configuration. The neutrino energy range used to calculate the total number of events is $10^{11} - 5 \times 10^{14}$ eV, comparible to what was assumed in the model. For non persistent but flaring sources, the parameters of the model were estimated for flares observed before IceCube construction. Hence the time-dependent upper limits are calculated averaging over a duration equal to the model flare during 40-string data taking (indicated as MUL in the legend). LS I $+61°$ 303 is assumed to be a periodic flaring source in a high state during 26% of the orbit.

## REFERENCES

Abbasi, R., et al. 2009a, ApJ, 701, L47

—. 2009b, Nucl. Inst. & Meth. in Phys. Res., A601, 294

—. 2010a, Nucl. Inst. & Meth. in Phys. Res., A618, 139

—. 2010b, *Time-Dependent Searches for Point Sources of Neutrinos with the 40-String and 22-String Configurations of IceCube*, subm. to ApJ

—. 2011, ApJ, 732, 18

Abdo, A. A., et al. 2009a, ApJ, 701, L123

—. 2009b, Science, 326, 1512

Acciari, V., et al. 2009, ApJ, 700, 1034

Acciari, V. A., et al. 2008, ApJ, 679, 1427

Achterberg, A., et al. 2006, A&A, 26, 155

Aharonian, F., et al. 2005a, A&A, 442, 1

—. 2005b, Science, 309, 746

Albert, J., et al. 2006, Science, 312, 1771

—. 2007, ApJ, 665, L51

—. 2009, ApJ, 693, 303

Athar, H., Jeżabek, M., & Yasuda, O. 2000, Phys. Rev. D, 62, 103007

Bosch-Ramon, V., Paredes, J. M., Romero, G. E., & Ribó, M. 2006a, A&A, 459, L25

Bosch-Ramon, V., Romero, G. E., & Paredes, J. M. 2006b, A&A, 447, 263

Braun, J., et al. 2008, Astropart. Phys., 29, 299

—. 2010, Astropart. Phys., 33, 175

Brocksopp, C., Tarasov, A. E., Lyuty, V. M., & Roche, P. 1998, A&A, 343, 861

Casares, J., Ribas, I., Paredes, J., Marti, J., & Allende Prieto, C. 2005, MNRAS, 360, 1105

Casares, J., Ribó, M., Ribas, I., Paredes, J. M., Martí, J., & Herrero, A. 2005, MNRAS, 364, 899

Chernyakova, M., Neronov, A., & Ribordy, M. 2009, eConf C091122

Chernyakova, M., Neronov, A., & Walter, R. 2006, MNRAS, 372, 1585

Christiansen, H. R., Orellana, M., & Romero, G. E. 2006, Phys.Rev., D73, 063012

Conrad, J., Botner, O., Hallgren, A., & Perez de los Heros, C. 2003, Phys.Rev., D67, 012002

Distefano, C., Guetta, D., Waxman, E., & Levinson, A. 2002, ApJ, 575, 378

Dubus, G., Cerutti, B., & Henri, G. 2010, A&A, 516, A18

Feldman, G. J., & Cousins, R. D. 1998, Phys. Rev. D, 57, 3873

Gregory, P. C., Peracaula, M., & Taylor, A. R. 1999, ApJ, 520, 376

Gregory, P. C., & Taylor, A. R. 1978, Nature, 272, 704

Gregory, P. C., et al. 1979, Astron. J., 84, 1030

Harrison, F. A., Ray, P. S., Leahy, D. A., Waltman, E. B., & Pooley, G. G. 2000, ApJ, 528, 454

Hill, G. C. 2003, Phys.Rev., D67, 118101

Hill, G. C., Hodges, J., Hughey, B., Karle, A., & Stamatikos, M. 2005, Examining the balance between optimising an analysis for best limit setting and best discovery potential, prepared for PHYSTATO5: Statistical Problems in Particle Physics, Astrophysics and Cosmology, Oxford, England, United Kingdom, 12-15 Sep 2005

Hillwig, T. C., & Gies, D. R. 2008, ApJ, 679, 1427

Hutchings, J. B., & Crampton, D. 1981, PASP, 93, 486

McClintock, J. E., et al. 2003, ApJ, 593, 435

Neil, E. T., Bailyn, C. D., & Cobb, B. E. 2007, ApJ, 657, 409

Neronov, A., & Ribordy, M. 2009, Phys. Rev. D, D79, 043013

Orellana, M., & Romero, G. 2007, Astrophys.Space Sci., 309, 333

Paredes, J. M., Martí, J., Ribó, M., & Massi, M. 2000, Science, 288, 2340

Ribó, M., Paredes, J. M., Moldón, J., Martí, J., & Massi, M. 2008, A&A, 481, 17

Romero, G. E., Okazaki, A. T., Orellana, M., & Owocki, S. P. 2007, A&A, 474, 15

Sidoli, L., Pellizzoni, A., Vercellone, S., Moroni, M., Mereghetti, S., & Tavani, M. 2006, A&A, 459, 901

Sierpowska-Bartosik, A., & Torres, D. F. 2009, ApJ, 693, 1462

Tavani, M., & Arons, J. 1997, ApJ, 477, 439

Tilav, S., et al. 2009, in Proc. of the 31st Int. Cosmic Ray Conf, Lodz, Poland, *Atmospheric Variations as observed by IceCube*, arXiv:1001.0776

Torres, D. F., & Halzen, F. 2007, A&A, 27, 500

Webb, N. A., Naylor, T., Ioannou, Z., Charles, P. A., & Shahbaz, T. 2000, MNRAS, 317, 528

Ziółkowski, J. 2005, MNRAS, 358, 851